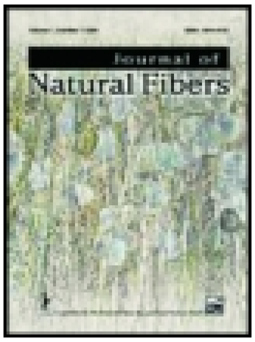

Journal of Natural Fibers

ISSN: 1544-0478 (Print) 1544-046X (Online) Journal homepage: http://www.tandfonline.com/loi/wjnf20

Effect of chopped/continuous fiber, coupling agent and fiber ratio on the mechanical properties of injection-molded jute/polypropylene composites

Sandhyarani Pailoor, H N Narasimha Murthy, Prakash Hadimani & T N Sreenivasa

To cite this article: Sandhyarani Pailoor, H N Narasimha Murthy, Prakash Hadimani & T N Sreenivasa (2018): Effect of chopped/continuous fiber, coupling agent and fiber ratio on the mechanical properties of injection-molded jute/polypropylene composites, Journal of Natural Fibers, DOI: 10.1080/15440478.2017.1410510

To link to this article: https://doi.org/10.1080/15440478.2017.1410510

Published online: 24 Jan 2018.

JOURNAL OF NATURAL FIBERS
https://doi.org/10.1080/15440478.2017.1410510

Check for updates

Effect of chopped/continuous fiber, coupling agent and fiber ratio on the mechanical properties of injection-molded jute/polypropylene composites

Sandhyarani Pailoor[a], H N Narasimha Murthy[b], Prakash Hadimani[c], and T N Sreenivasa[a]

[a]Department of Mechanical Engineering, AMC Engineering College, Bangalore, India; [b]Department of Mechanical Engineering, R V College of Engineering, Bangalore, India; [c]Research and Application Department, Steer Engineering, Bangalore, India

ABSTRACT

This paper presents the development of jute/polypropylene (PP) composites by twin-screw extrusion and injection molding. Jute/PP was compounded using twin-screw extruder and injection molded. The effects of chopped/continuous fibers, coupling agent and fiber ratio on mechanical properties were investigated. Tensile and flexural **moduli** of continuous jute/PP were greater than those of chopped fiber/PP. Tensile, flexural and impact strengths were greater in chopped fiber/PP along with elongation at break. Coupling agent improved the tensile and flexural strengths, and these increased with fiber content, whereas impact strength and elongation at break decreased with fiber loading. The results were analyzed using ANOVA and regression analyses.

摘要

介绍了双螺杆挤出成型技术在黄麻/聚丙烯复合材料中的应用。黄麻/聚丙烯采用双螺杆挤出机和注塑成型复合。研究了切碎/连续纤维、偶联剂和纤维比对机械性能的影响。连续黄麻/聚丙烯的拉伸模量和弯曲模量均大于短纤维/聚丙烯。短切纤维/聚丙烯的拉伸强度、弯曲强度和冲击强度随着断裂伸长率的增加而增大。偶联剂提高了纤维的拉伸强度和弯曲强度，随着纤维含量的增加而增加，而冲击强度和断裂伸长率随纤维负荷的增加而降低。结果用方差分析和回归分析进行分析。

KEYWORDS
Twin screw extruder; Injection Molding; Jute fibres; Mechanical properties; Regression Analysis; ANOVA

Introduction

The fabrication of natural fiber reinforced composites is challenging because of fiber handling and their intrinsic properties. The major advantages of natural fibers include excellent specific strength, low density (1.3–1.5 g/cm^3), low cost, biodegradability and vibration damping. Application of renewable resources and concern about the reduction of both greenhouse gases and CO_2 emissions drive plastic industries toward natural fibers. They reduce the wear of screws and barrels of plastic processing equipment compared with the commonly used glass fibers (Aggarwal et al. 2013; Bledzki et al. 2015; Ferreira et al. 2016).

While processing natural fibers, the main considerations are their hygroscopic behavior and low resistance to high temperature, which limit the choice of resins. Fortunately, the equipment and techniques used for natural fiber composites are relatively similar to those of conventional inorganic fiber composites, which make industries easily adopt natural fiber composites for different applications (Aggarwal et al. 2013). Use of well-compounded pellets in injection molding significantly improves the tensile strength and modulus of composites (Bledzki et al. 2015). Gunning et al. investigated the processing conditions of

CONTACT H N Narasimha Murthy hnmdatta@yahoo.com Department of Mechanical Engineering, R V College of Engineering, Bengaluru-560059, India.

Color versions of one or more of the figures in the article can be found online at www.tandfonline.com/wjnf.

polylactic acid (PLA)-based green composites via twin-screw extrusion. In the experiments, the tensile strength of jute/PLA yielded 82.2 MPa, which is the maximum reported to date for injection-molded specimens (Gunning et al. 2014).

Temperature, screw configuration and screw speed of twin-screw extruders influence the quality of the compounded pellets (Arao et al. 2015). The pellets produced using a low-temperature profile exhibited properties superior to those produced at high temperature, owing to the reduced thermal degradation of fibers during compounding (Gunning et al. 2014). Especially for natural fibers, thermal degradation occurs above 180°C, which is around the melting temperature of the matrix. To mitigate the thermal degradation of jute fiber during processing, the control temperature was set to 180°C. Higher screw speed leads to higher shear force during compounding, resulting in better fiber dispersion. Shear heating increases the temperature of the extruded compounds by 10–20 °C. To minimize thermal degradation by shear heating, the screw speed has to be maintained at around 150 rpm. In general, kneading elements can generate high shear stress during compounding and are often used to improve dispersion quality (Arao et al. 2015).

Jute is one of the most temperature-stable natural fibers compared with Kenaf, Abaca and wood microfibers (Aggarwal et al. 2013). Jute quickly absorbs high moisture in the range of 1000–3000 ppm (Doan, Brodowsky, and Mader 2007). During compounding, non-dried fibers undergo hydrolytic degradation instantaneously, which is 10,000 times faster than the thermal degradation caused by high temperature and 5000 times faster than the thermo-oxidative degradation caused by the presence of oxygen. Removal of moisture is required during the compounding and processing of jute either by air-drying (up to 100°C for 24 h) or vacuum degassing during extrusion (Yang et al. 2011). The disadvantages of air-drying include fiber handling, high time and cost along with fiber degradation. Thus, vacuum degassing was adopted to remove the moisture during the twin-screw extrusion process in this research.

End properties of the composites depend on the length, diameter, fiber ratio, orientation and distribution of the fibers in the matrix, which are dependent on the processing conditions (Puglia et al. 2008). Jute is polar in nature and is noncompatible with nonpolar thermoplastics like other bio-based lignocellulosic fibers. Differences in their polarity create challenge in the fiber–matrix interfacial adhesion, which restricts the load transfer between the polymer matrix and the fibers. In case of poor interfacial adhesion, the fibers act as fillers without contributing to the strength of the composites (Yan et al. 2013). Addition of a coupling agent is one of the known effective ways of improving the interfacial adhesion between bio-fibers and thermoplastics (George et al. 2012). A wide variety of chemicals has been explored as coupling agents. Among these, maleic anhydride grafted polypropylene (MAPP) is one of the most popular and extensively studied coupling agents for bio-fiber/thermoplastic composites. MAPP improves interfacial adhesion between thermoplastic and fiber and thus improves the mechanical properties of the composites (Aggarwal et al. 2013).

Review of the literature suggested that the mechanical properties of natural fiber/thermoplastic composites are controlled by process parameters, fiber type, fiber ratio and fiber–matrix interface. Many authors adopted preheating and the chemical treatment of fibers, which is cost inhibitive. Adoption of vacuum degassing for moisture removal during extrusion has been scarcely addressed. Vacuum degassing can effectively eliminate fiber drying, chemical treatment and thermal degradation. The effects of chopped/continuous fibers, coupling agent and fiber content on the mechanical properties of jute/PP using twin-screw extruder and injection molding have been scarcely reported. In the present research, temperature (180 °C), screw configuration (kneading blocks) corresponding to optimum shear during extrusion and screw speed (150 rpm) were adopted based on standard practice in the industry. The effects of MAPP as a coupling agent and fiber content (20, 30 and 40 wt.%) in PP were investigated using design of experiments.

Materials and characterization

Materials

Polypropylene (PP) homopolymer Repol (PP AM650N) pellets, with melting point 180°C, melt flow rate 65 g/10 min at 190°C/2.16 kg (MFI 65, Reliance Polymer) and combed raw jute fibers were procured from Reliance Polymer (India) and Uma Jute Twine Mills (India), respectively. The coupling agent – maleic acid anhydride grafted co-polymer (MAPP), type Fusabond® P series (M-613–05) – was procured from Du Pont (India), with a graft level of 1.4%, melting point 162 °C and melt flow rate 120 g/10 min (190 °C, 2.16 kg).

Fabrication of composites

The combed raw jute fibers were directly fed through the extruder for continuous fiber/PP compounding. Similarly, combed fibers were fed into the jute cutter to make chopped fibers of 1–2 mm length and then fed to the extruder for chopped fiber/PP compounding. Pellets of PP were blended with 2 wt% MAPP in a container for 10 min at constant speed for preparing one set of specimens. As-procured PP pellets were used for preparing another set of specimens. Jute/PP pellets were prepared using twin-screw co-rotating extruder (STEER Omega-40) operated in co-rotating intermeshing self-wiping mode with throughput between 50 and 150 kg/h. The extruder comprised eight temperature-controlled barrels as shown in Figure 1.

The pellets were fed through the main volumetric feeder to the intake barrel, which is provided with water-cooling jackets. It moves through the conveying elements to the kneading block in which polymer melting takes place. Jute fiber fed through the side volumetric feeder mixes with the molten PP. Both mixing and distribution of fibers take place in this section. The compounded material is transferred to the vacuum section from which all the volatiles are evacuated. Vacuum vent inserts are mounted lateral to the extruder barrels to improve the volatile removal rate, reduce voids and increase the production rate. The compounded jute/PP melt strands were quenched in a water bath, surface dried in the air knife before cutting into 2×2 mm^2 pellets in the pelletizer. The pellets were dried for four hours at 100°C and injection molded.

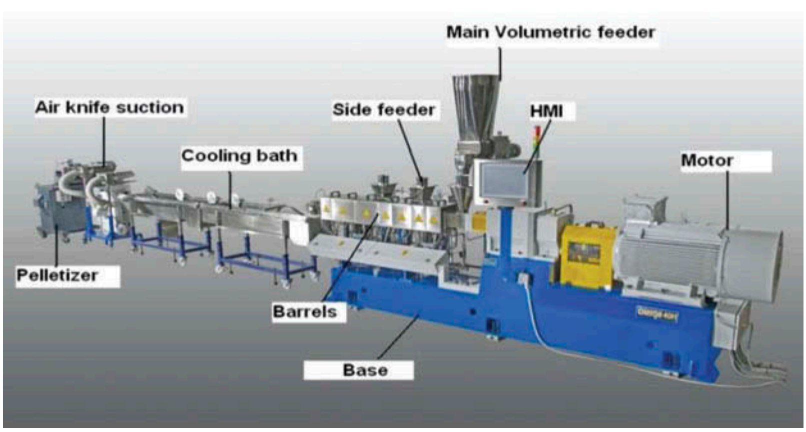

Figure 1. Twin-screw extruder OMEGA 40.

Table 1. Experimental factors, levels and responses.

		Factor Level			
Factor	Code	L_1	L_2	L_3	Degree of Freedom
Resin/fiber ratio	A	80: 20	70: 30	60: 40	2
Fiber	B	Continuous (CNJF)	Chopped (CHJF)	-	1
Coupling agent	C	With (WCA)	Without (NCA)	-	1

Experimental Responses						
Tensile properties			Flexural properties		Impact Strength	
Strength, (TS) MPa	Modulus, (TM) GPa	Elongation at break, (EB) %	Strength, (FS) MPa	Modulus, (FM) GPa	Un-Notched, (UNIS) J/m	Notched, (NIS) J/m

Experimental details

Experimental factors and levels along with experimental responses are presented in Table 1 for L_{12} full factorial design with five replicates.

Mechanical characterization

Tensile tests were performed on 165 × 19 x 3.2 mm^3 specimens as per ASTM D638 using Universal Testing Machine, Model–5569 A, Instron, with a strain rate of 5 mm/min. Three-point static flexural tests were performed on 127 × 12.7 x 3.2 mm^3 specimens as per ASTM D790 using the same UTM at a crosshead speed of 5 mm/min. Flexural strength and modulus were calculated using equations (1) and (2):

$$\text{Flexural strength, FS} = \frac{3PL}{2bd^2} \tag{1}$$

$$\text{Flexural modulus, FM} = \frac{PL^3}{4\delta bd^3} \tag{2}$$

where P is the maximum load, L is the length between supports, b and d are width and thickness of specimens, respectively, and δ is the deflection at load P.

Notched and un-notched (64 x 3.2 x 12.7 mm^3) specimens with a 2.5-mm-deep triangular notch at the mid-edge were tested as per ASTM D256 using an impact testing machine – Pendulum Impact Tester, Model – Impactor 2, CEAST Italy.

Scanning electron microscopy

Tensile fractured surfaces of the specimens were examined using a scanning electron microscope (Hitachi SU 1500) at an accelerating voltage of 5 and 15 KV and an emission current of 86000 nA to study the interfacial bonding between jute fiber and PP.

Results and discussion

Tensile properties

The mean responses of the five replicates are presented in Table 2. Tensile strength of the composites increased with increase in fiber content from 20 to 40 wt% irrespective of the type of fiber and application of a coupling agent. Other reports suggest an increase in tensile strength only when a coupling agent is used in the composites (Bledzki et al. 2015; Cabrera et al. 2012; Pickering, Efendy, and Le 2016). In the present research, the improvement in tensile strength is attributed to both twin-screw extrusion and coupling agent. The load is effectively transferred from the matrix to the fiber.

The addition of MAPP increased the tensile strength of the composites with fiber loading. Maleic anhydride group forms covalent and hydrogen bonds with the hydroxyl groups of the

Table 2. Experimental results with mean of the responses.

	Factors			Responses						
Run	A	B	C	TS	TM	EB	FS	FM	NIS	UNIS
1	80:20	CNJF	WCA	36.45	3.74	2.165	63.67	3.25	30.87	199
2	80:20	CHJF	WCA	40.65	3.94	2.827	66.72	3.00	37.69	286.96
3	80:20	CNJF	NCA	31.27	3.57	2.652	54.662	3.07	38	268.3
4	80:20	CHJF	NCA	33.27	3.46	3.341	56.21	2.67	41.39	338.03
5	70:30	CNJF	WCA	38.72	4.49	1.695	71.202	4.01	36.5	211.15
6	70:30	CHJF	WCA	43.33	3.70	3.198	69.83	3.04	41.29	321.05
7	70:30	CNJF	NCA	32.23	4.89	1.718	56.169	4.12	38.63	218.95
8	70:30	CHJF	NCA	33.69	3.37	3.449	57.81	2.95	44.99	259.26
9	60:40	CNJF	WCA	40.89	5.06	1.699	69	4.73	36.66	179.5
10	60:40	CHJF	WCA	44.00	5.03	2.212	74.82	3.92	37.16	233.9
11	60:40	CNJF	NCA	32.25	5.32	1.711	56.08	4.62	41.8	179.44
12	60:40	CHJF	NCA	33.28	5.11	2.275	57.91	4.05	42.71	231.18

fiber (Hossain et al. 2010; Panaitescu et al. 2010). This causes better adhesion between the fiber and the matrix and leads to improvement in tensile strength (Beheraa et al. 2012) . Increase in tensile strength from 31.27 to 44 MPa in the present work is superior to the values reported elsewhere (23–35 MPa) of Franco Marques et al. (2011). In general, as the fiber content increases, gathering of fibers takes place instead of dispersion (Beheraa et al. 2012). Injection molding yields more homogeneity and the fibers can serve as effective reinforcement to the matrix, which induces stiffening effect and improves tensile strength. The influence of fiber loading, coupling agent and fiber type on tensile strength of the specimens is shown in Figure 2 (a).

The tensile modulus of jute/PP composites increases with fiber content and the addition of a coupling agent. Stiffening effect occurs due to the better fiber wetting and fiber distribution. Deformation of PP strongly depends on its molecular weight. As the fiber content increases, the degree of obstruction increases and it also restricts the mobility of PP, which increases the stiffness of the composites, resulting in improved tensile modulus (Rana et al. 1998). The addition of MAPP improved the tensile modulus in all the composites due to the presence of hydroxyl groups. Chopped fiber composites are superior to continuous fiber specimens only when a coupling agent is used. Tensile modulus of the composites increased nominally with increase in the fiber content.

Elongation at break decreased with increase in fiber content. Fibers obstruct the mobility of PP chains avoiding large movements due to stresses (Rana et al. 1998), inducing the break of specimens at lower values of deformation. Generally, as strength increases, elongation at break decreases, and vice versa. A higher strength means it is hardly deformed and breaks at low strain. Poor fiber–matrix adhesion at the interface may weaken the composite, and fibers may behave not

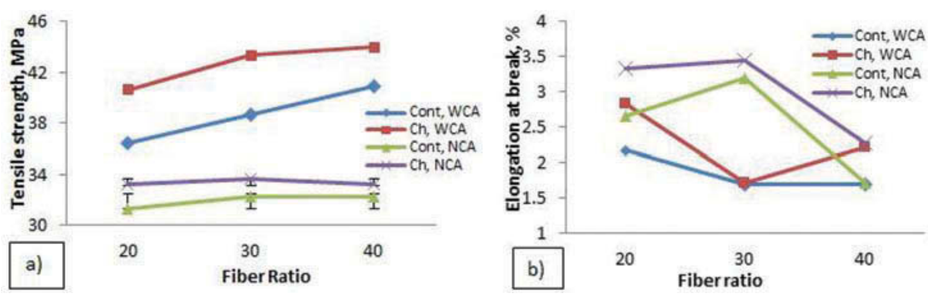

Figure 2. Influence of fiber type, fiber ratio and coupling agent on a) tensile strength and b) elongation at break of jute/PP.

as reinforcements but as defects in the matrix. In these situations, strength is lowered and elongation at break increases.

In case of specimens without a coupling agent, elongation at break increased in continuous and chopped fiber composites and it was the highest at 30 wt% fiber content. In contrast, it was the lowest in composites with the same fiber content processed with a coupling agent as shown in Figure 2 (b).

Flexural properties

The flexural behavior of the composites was similar to that of tensile behavior. The variations in flexural strength and modulus are summarized in Figure 3 (a) and 3 (b). The homogenous distribution of fibers in the matrix contributed to improvement in flexural strength. In the present research, flexural strength varied from 54.66 to 74.82 MPa, which is much superior to that reported elsewhere, with a maximum of 58 MPa for the same fiber (Rana et al. 1998). Flexural strength increased with increase in the fiber content by 8.1 MPa and the use of a coupling agent increased the same by 16.91 MPa.

Flexural modulus increased with increase in fiber content, but the addition of a coupling agent in the chopped fiber composites showed maximum flexural modulus at 30% fiber content. Flexural modulus was superior in continuous fiber composites compared to that of chopped fiber composites. Fiber entanglement may also reduce the flexural modulus.

Izod impact test results

Notched and un-notched experiments were carried out for determining the capacity of the composites against impact stresses. The notched impact test helps characterize the energy of crack propagation and the un-notched test, for crack initiation and crack propagation. The results of both the assays are

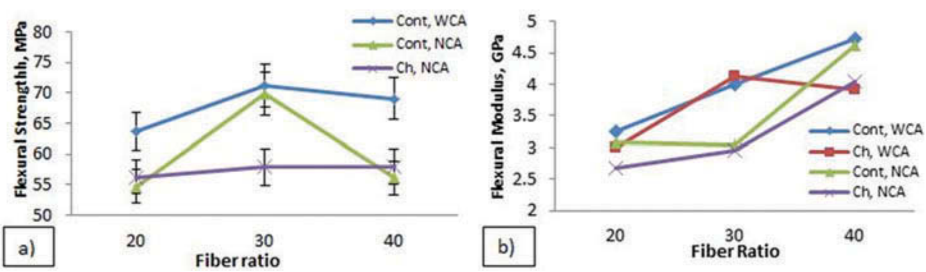

Figure 3. Influence of fiber type, fiber ratio and coupling agent on a) flexural strength and b) flexural modulus of jute/PP.

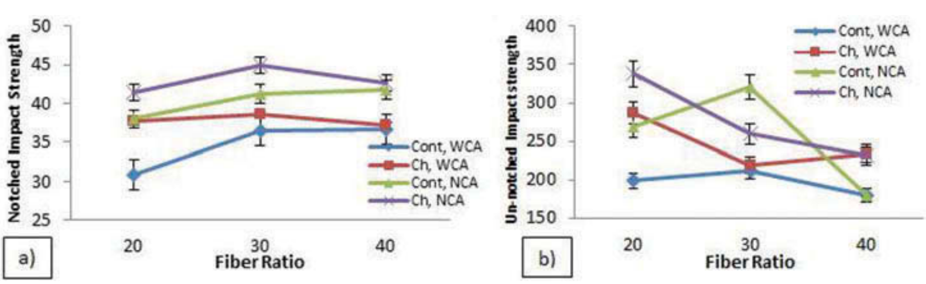

Figure 4. Influence of fiber type, fiber ratio and coupling agent on a) notched impact strength and b) un-notched impact strength of jute/PP.

summarized in Figure 4 (a) and 4 (b). The composite specimens of the present study showed higher impact energy than that of PP (25 J/m). The impact energy of the composites improved with increase in fiber content from 20 to 30 wt%. However, it decreased for the 40 wt% fiber composites. This effect is related to increasing the heterogeneity on the surface of the composite with increase of fibers, as it increases the points of stress and hence the possibility of fracture. The composites modified with a coupling agent exhibited less impact strength in both continuous and chopped fiber specimens, which is in contradiction to the observations of Franco Marques et al. (2011). Notched impact strength of chopped fiber composites was superior to that of continuous fiber specimens. Fiber entanglement contributes to reducing the impact strength. Increase in impact strength in the present work is superior to that reported elsewhere (26.9 J/m for 30% jute fiber) (Rana et al. 1998).

Increase in impact energy in the un-notched specimens was significant compared to that of the notched one. Un-notched impact strength of the composites decreased steadily with increase in chopped fiber content. This is in agreement with the results reported by many authors on jute and bio-based fibers (Aggarwal et al. 2013). Impact energy increased with increase in continuous fiber from 20% to 30% and decreased for 40 wt%. It was commonly observed in composites with or without a coupling agent. The initial increase of impact energy indicates that mechanical interlocking was good enough to transfer small loads from the matrix to the fiber. As the fiber percentage increased, the impact strength decreased for the same reason. In chopped fibers, this energy decreased with increasing percentage of fibers. This interesting result was related to the presence of many fiber ends within the body of the composites; it causes crack initiation and hence potential composite failure. Addition of fibers also increased the probability of fiber agglomeration, creating regions of stress concentration that required less energy to initiate a crack. Good improvement in un-notched strength was observed (179.44–338 J/m) in the present research compared with other studies (110–122 J/m) (Rana et al. 1998).

Signal-to-noise (S/N) ratio

The experimental responses were transformed to S/N ratios based on larger-the-better quality characteristic for each response (Bharti and Khan 2010). The treatment combination resulting in the highest S/N ratio corresponds to least variability in the response. The S/N ratio was computed using equation (3) as per Cabrera et al. (2012).

$$\frac{S}{N} = -10\log_{10}\left[\frac{1}{N}\sum\frac{1}{Y_i^2}\right] \tag{3}$$

where Yi is observations, N is number of replications and i is 1 to N.

The repeatability of the measurements is implicitly studied by considering five replications. The S/N ratio of five replicates for the responses is presented in Table 3.

The normal probability plots were examined for log (s) and S/N ratio for each of the responses to study the stability of the process. The plots for the responses were also examined and the data was found to be in good fit for normal distribution in all the cases.

Figure 5 shows the interaction plots of the responses with respect to the S/N ratio, which helps enter the optimal parametric combination.

ANOVA of responses

ANOVA for tensile strength is presented in Table 4. It indicates that coupling agent and fiber type are significant when compared with the resin to fiber ratio.

Similarly, ANOVA was performed for each of the responses, and significant factors for different responses are presented in Table 5.

Table 3. Signal to noise (S/N) ratio for the response factors.

	Factors			S/N Ratio						
Expt. No	A	B	C	TS	TM	EB	FS	FM	NIS	UNIS
1	20	CNJF	WCA	31.234	11.458	6.709	36.079	10.241	29.791	45.977
2	20	CHJF	WCA	32.181	11.919	9.027	36.485	9.531	31.525	49.156
3	20	CNJF	NCA	29.903	11.053	8.471	34.754	9.751	31.596	48.572
4	20	CHJF	NCA	30.441	10.774	10.478	34.996	8.522	32.338	50.579
5	30	CNJF	WCA	31.759	13.050	4.583	37.050	12.063	31.246	46.492
6	30	CHJF	WCA	30.165	13.789	4.700	34.990	12.299	31.738	46.807
7	30	CNJF	NCA	32.736	11.362	10.098	36.881	9.645	32.317	50.131
8	30	CHJF	NCA	30.550	10.565	10.754	35.240	9.405	33.062	48.275
9	40	CNJF	WCA	32.232	14.091	4.604	36.777	13.506	31.284	45.081
10	40	CHJF	WCA	32.869	14.032	6.896	37.480	11.868	31.402	47.381
11	40	CNJF	NCA	30.171	14.523	4.665	34.976	13.286	32.424	45.078
12	40	CHJF	NCA	30.444	14.174	7.140	35.255	12.156	32.611	47.279

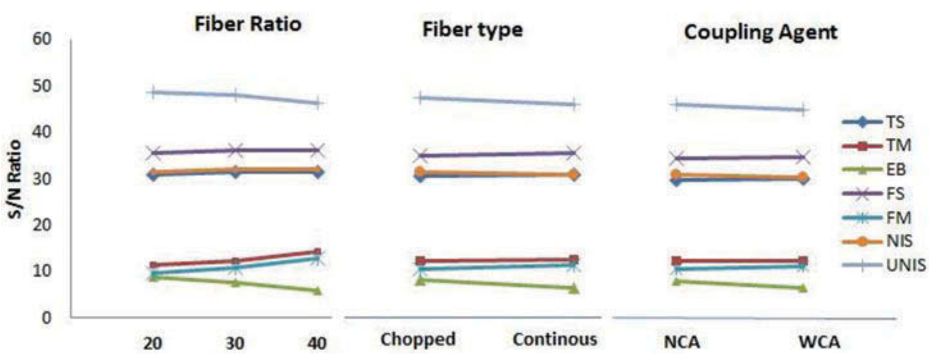

Figure 5. Interaction plots of different responses using S/N ratio with respect to fiber ratio, fiber type and coupling agent of jute/PP.

Table 4. ANOVA for tensile strength of jute/PP composites.

Source	Sum of Squares	Df	Mean Square	F-value	*p*-value Prob > F	Significance
A-Fiber ratio	10.26	2	5.132	3.20	0.103	-
B-Fiber type	22.44	1	22.441	14.00	0.007	Significant
C-Coupling agent	192.40	1	192.400	120.01	0.000	Significant
Residual	11.22	7	1.603			-
Cor Total	236.33	11				-

Table 5. Results of ANOVA of all the responses.

Significant Factors for the Experimental Responses		
Resin to fiber ratio	Fiber type	Coupling agent
Tensile Modulus	Tensile Strength	
Elongation at break	Elongation at break	Tensile Strength
Flexural Strength	Flexural Modulus	Flexural Strength
Flexural Modulus	Notched Strength	Notched Strength
Un-Notched Strength	Un-Notched Strength	

Regression models

Relations between the experimental parameters and the responses were developed using Regression models using Minitab 17. The factors are coded with numeric values to simplify the regression

Table 6. Relation between the regressors and the responses.

Regression equations	R^2 (%)	Experimental	Predicted
TS = 42.38 + 1.097 A + 2.735 B - 8.008 C	94.99	44	43.133
TM = 3.529 + 0.727 A - 0.410 B - 0.040 C	77.61	5.32283	5.22
EB = 1.431–0.386 A + 0.944 B + 0.225 C	81.92	3.45	2.997
FS = 74.67 + 2.068 A + 2.09 B - 12.73 C	94.19	74.82	72.324
FM = 3.446 + 0.6672 A - 0.697 B - 0.078 C	92.65	4.73453	4.6726
NIS = 23.85 + 1.297 A + 3.80 B + 4.56 C	78.04	44.99	43.164
UNIS = 191.6–33.53 A + 69.0 B + 10.6 C	79.33	338.03	317.27

model. Resin to fiber ratio is coded as 1, 2 and 3, indicating the resin to fiber ratios of 80:20, 70:30 and 60:40, respectively. Continuous fiber and with coupling agent is coded as 1. Chopped fiber and without coupling agent is coded as 2 in the model.

The relation between the regressors and the response is given in Table 6. Equations in Table 6 were used to estimate the responses. The predicted and experimental responses closely agree with each other. Values of R^2 indicated that the quadratic model was acceptable as the statistical model with maximum error of 13%.

Morphological characterization

Tensile fractured jute/PP specimens were examined for interfacial bonding. SEM micrographs revealed superior fiber/matrix bonding, good fiber wetting and uniform fiber distribution in all the specimens due to the incorporation of kneading elements in the twin-screw extruder, which resulted in higher tensile strength. Reduced micropores or voids are due to vacuum degassing during the fabrication, resulting in superior strength compared with the results reported in the open literature. Fiber pullout and debonding without adherence to the matrix dominated in the fracture surfaces (Figure 6(b)) of the specimens without the coupling agent, compared with those shown in Figure 6 (a), which improves the specimens with coupling agent. The micrograph (Figure 6 (c))

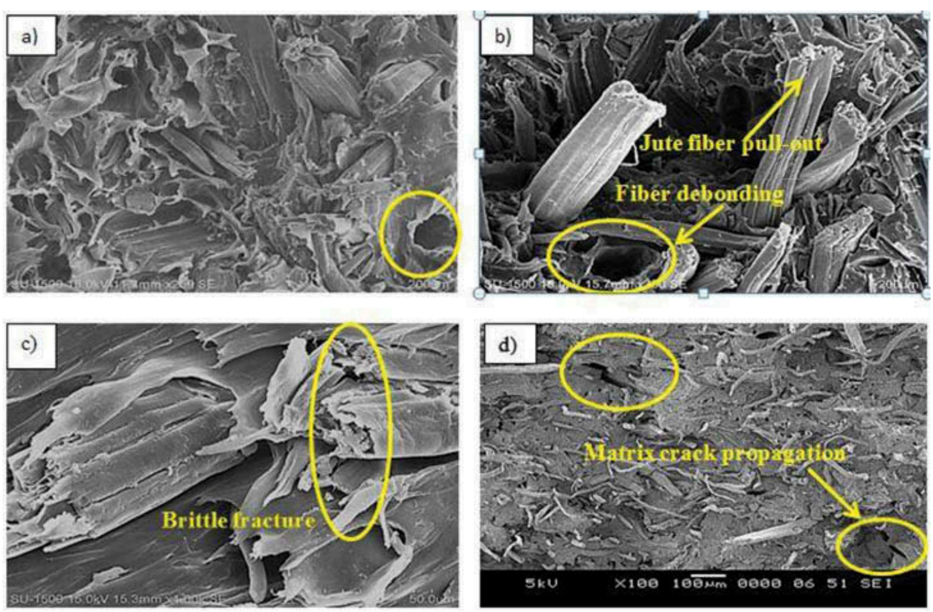

Figure 6. SEM micrographs of tensile fractured specimens (a) continuous fiber, with coupling agent, (b) continuous fiber, without coupling agent, **(c) chopped fiber, with coupling agent** and (d) chopped fiber, without coupling agent specimen.

showed brittle failure of the specimens, as evidenced by the fiber breakage. Crack initiation and propagation through the matrix were observed in Figure 6 (d). The presence of a coupling agent and fiber type at the fractured surface suggests its contribution to the load bearing and hence improvement in the mechanical properties. SEM observations confirmed that the coupling agent influenced the tensile strength significantly.

Conclusion

The effect of chopped/continuous jute fibers, MAPP coupling agent and fiber content in PP was investigated by fabricating pellets using a twin-screw extruder and testing specimens using injection molding. Vacuum degassing was adopted during compounding instead of fiber drying and chemical treatment. The tensile strengths of both continuous and chopped fiber composites processed without a coupling agent increased with increase in fiber content. However, the coupling agent improved the tensile and flexural strengths of the composites by 9.64 MPa and 16.91 MPa. Tensile and flexural moduli of continuous fiber/PP were greater than those of chopped fiber/PP. Tensile, flexural and impact strengths and elongation at break were greater in chopped fiber/PP than those in continuous fiber/PP. Tensile and flexural strengths and moduli increased, and impact strength and elongation at break decreased with increase in fiber content. Maximum tensile modulus of 5.32 GPa was obtained in continuous fiber composites processed without a coupling agent and its improvement was 4.1GPa. Chopped fiber composites with fiber content 20 wt% processed without a coupling agent showed the highest elongation at break. The highest flexural strength of 74.82 MPa was observed in chopped fiber composites processed with a coupling agent. Its improvement was 43 MPa. The highest flexural modulus of 4.73 GPa was observed in 40 wt% continuous fiber composites processed with a coupling agent and its improvement was 3.4 GPa. Notched impact strength of 44.99 J/m was observed in 30 wt% chopped fiber composites processed without a coupling agent and its improvement was 20 J/m. All the improvements are with respect to those of PP specimens. ANOVA was used to identify the most influencing factors and SEM was used to study interfacial bonding.

References

Aggarwal, P. K., N. Raghu, A. Karmarkar, and S. Chuahan. 2013. Jute polypropylene composites using m-TMI-grafted-polypropylene as a coupling agent. *Materials & Design* 43:112–17. doi:10.1016/j.matdes.2012.06.026.

Arao, Y., T. Fujiura, S. Itani, and T. Tanaka. 2015. Strength improvement in injection-molded jute-fiber-reinforced polylactide green-composites. *Composites Part B: Engineering* 68:200–06. doi:10.1016/j.compositesb.2014.08.032.

Beheraa, A., S. Avanchaa, R. Basaka, R. Senb, and B. Adhikari. 2012. Fabrication and characterizations of biodegradable jute reinforced soy based green composites. *Carbohydrate Polymers* 88:329–35.

Bharti, P. K., and M. I. Khan. 2010. Recent methods for optimization of plastic injection molding process-A retrospective and literature review. *International Journal of Engineering Science and Technology* 2 (9):4540–54.

Bledzki, A. K., P. Franciszczak, Z. Osman, and M. Elbadawi. 2015. Polypropylene bio composites reinforced with softwood, abaca, jute and kenaf fibers. *Industrial Crops and Products* 70:91–99.

Cabrera, F. F. D., I. Hanafi, A. Khamlichi, and A. Jabbouri. 2012. Multi-criteria Optimization Using Taguchi and Grey Relational Analysis in CNC Turning of PEEK CF30. *Journal of Thermoplastic Composite Materials* 25:101–14.

Doan, T., H. Brodowsky, and E. Mader. 2007. Jute fiber/polypropylene composites II. Thermal, hydrothermal and dynamic mechanical behavior. *Composites Science and Technology* 67:2707–14.

Ferreira, J. M., C. Capela, J. Manaia, and J. D. Costa. 2016. Mechanical properties of Woven Jute/Epoxy composites. *Materials Research* 19 (3):702–10.

George, G., E. T. Jose, K. Jayanarayanan, E. R. Nagarajan, M. Skrifvars, and K. Joseph. 2012. Novel bio-commingled composites based on jute/polypropylene yarns: Effect of chemical treatments on the mechanical properties. *Composites: Part A* 43:219–30.

Gunning, M. A., L. M. Geever, J. A. Killion, J. G. Lyons, and C. L. Higginbotham. 2014. The effect of processing conditions for polylactic acid based fiber composites via twin-screw extrusion. *Journal of Reinforced Plastic Composites* 33:648–62.

Hossain, M. K., M. W. Dewan, M. Hosur, and S. Jeelani. 2010. Mechanical performances of surface modified jute fiber reinforced biopol nanophased green composites. *Composite Part B* 42:1701–07.

Marques, E. F., J. A. Mendez, M. A. Pelach, F. Vilaseca, J. Bayer, and P. Mutje. 2011. Influence of coupling agents in the preparation of polypropylene composites reinforced with recycled fibers. *Chemical Engineering Journal* 166:1170–78.

Panaitescu, D. M., M. D. Iorga, S. Serban, and A. N. Frone. 2010. Composite materials of polypropylene and waste jute fibers. *Material Plastic* 47 (1):1–4.

Pickering, K. L., M. G. A. Efendy, and T. M. Le. 2016. A review of recent developments in natural fiber composites and their mechanical performance. *Composites Part A: Applied Science and Manufacturing* 83:98–112.

Puglia, D., A. Terenzi, S. E. Barbosa, and J. M. Kenny. 2008. Polypropylene – Natural fiber composites. Analysis of fiber structure modification during compounding and its influence on the final properties. *Composite Interfaces* 15 (2–3):111–29.

Rana, A. K., A. Mandal, B. C. Mitra, R. Jacobson, R. Rowell, and A. N. Banerjee. 1998. Short Jute fiber-reinforced polypropylene composites: Effect of compatibilizer. *Journal of Applied Polymer Science* 69:329–38.

Yan, Z. L., H. Wang, K. T. Lau, S. Pather, J. C. Zhang, G. Lin, and Y. Ding. 2013. Reinforcement of polypropylene with hemp fibers. *Composites: Part B* 46:221–26.

Yang, Y., T. Ota, T. Morii, and H. Hamada. 2011. Mechanical property and hydrothermal aging of injection molded jute/polypropylene composites. *Journal of Material Science* 46:2678–84.